SCIENTIFIC REPORTS

SUBJECT AREAS:
SCIENTIFIC DATA
ELECTRONIC PROPERTIES AND DEVICES
TWO-DIMENSIONAL MATERIALS
ELECTRONIC AND SPINTRONIC DEVICES

Received
22 March 2013

Accepted
15 April 2013

Published
3 May 2013

Correspondence and requests for materials should be addressed to N.W. (phwang@ust.hk)

* These authors contributed equally to this work.

Density of States and Its Local Fluctuations Determined by Capacitance of Strongly Disordered Graphene

Wei Li[1,2]*, Xiaolong Chen[1]*, Lin Wang[1], Yuheng He[1], Zefei Wu[1], Yuan Cai[2], Mingwei Zhang[1], Yang Wang[1], Yu Han[1], Rolf W. Lortz[1,2], Zhao-Qing Zhang[1,2], Ping Sheng[1,2] & Ning Wang[1,2]

[1]Department of Physics, [2]the William Mong Institute of Nano Science and Technology, the Hong Kong University of Science and Technology, Clear Water Bay, Kowloon, Hong Kong, China.

We demonstrate that fluctuations of the local density of states (LDOS) in strongly disordered graphene play an important role in determining the quantum capacitance of the top-gate graphene devices. Depending on the strength of the disorder induced by metal-cluster decoration, the measured quantum capacitance of disordered graphene can dramatically decrease in comparison with pristine graphene. This is opposite to the common belief that quantum capacitance should increase with disorder. To explain this counterintuitive behavior, we present a two-parameter model which incorporates both the non-universal power law behavior for the ADOS and a lognormal distribution of LDOS. We find excellent quantitative agreements between the model and measured quantum capacitance for three disordered samples in a wide range of Fermi energies. Thus, by measuring the quantum capacitance, we can simultaneously determine the ADOS and its fluctuations. It is the LDOS fluctuations that cause the dramatic reduction of the quantum capacitance.

For disordered graphene, theoretical predictions suggest that as the disorder strength increases, the average density of states (ADOS) increases accordingly, in comparison with pristine graphene[1,2]. The changes of the ADOS near the charge neutrality point (NP) still remain ambiguous and under debate[3–9]. One of the theoretical predictions on disordered graphene suggested that the ADOS followed a power law, i.e. $\langle\rho(E_F)\rangle \sim |E_F|^{\alpha}$, $0 < \alpha < 1$, where E_F is the Fermi energy[3,4] and the exponent α decreases with increasing disorder . Thus, the ADOS is expected to increase when disorder becomes stronger in graphene.

In two-dimensional (2D) materials, quantum capacitance[10,11] C_q can directly reflect the ADOS because it is proportional to the ADOS at E_F due to the large contribution of electron compressibility[12], i.e. $C_q = e^2 \cdot \langle\rho\rangle$, where e is the electron charge and $\langle\rho\rangle$ is the ADOS at E_F. The measurement of C_q is more immune to the scatterings arising from disorder compared to the DC transport measurement. The theoretical expressions of the quantum capacitance and the ADOS in single layer pristine graphene[11,13] have been verified experimentally by capacitance measurements for devices with various top-gate geometries[14–17].

The measurement of quantum capacitance is expected to help probe the non-conducting states, particularly in strong localization systems such as the chemically decorated graphene structures, which contain strong disorder as evidenced by the DC transport measurement[18–23]. So far, no experimental work seems to have been reported on the quantum capacitance of disorder graphene. Since the ADOS has been predicted to increase in disordered graphene, it is natural to expect that quantum capacitance measurements should reflect the increased ADOS directly.

On the other hand, the local density of states (LDOS) in disordered graphene nanostructures has been investigated theoretically and experimentally (mostly by scanning tunneling microscopy), and it is believed to fluctuate due to the presence of the disorder[24–29]. For substrate-supported pristine graphene, experimental works demonstrated that the spatial fluctuations of LDOS in the vicinity of the NP follow Gaussian distributions[30,31]. Gaussian distributions have been predicted for weakly disordered systems with extended states[32]. However, for strongly disordered systems, the fluctuations of LDOS have been predicted to be lognormal[33]. Recent numerical simulations showed the lognormal distribution in disordered graphene[34]. The lognormal distribution has also been identified in some experimental studies of 2D materials[35].

To introduce strong disorder into single layer graphene, we adopted our previously developed method of Ag-decoration of graphene surfaces[18]. Through transport measurements of Ag-decorated graphene, we found strong

Anderson localization induced by the disorder of Ag clusters. The resistance of Ag-decorated graphene largely increased right after the decoration, and the variable-range-hopping (VRH) model interpreted the experimental data of graphene conductivity fairly well even at the temperature as high as 300 K[18]. Obviously, strong localization had been induced in such disordered graphene even at room temperature. It should be pointed out that the Ag decoration method was proved by the comparison experiments to be non-invasive and the lattice of graphene was preserved. Therefore, it makes strongly disordered Ag-decorated graphene an interesting candidate for the study of both the ADOS and its local fluctuations through capacitance measurements.

In this letter, contrary to our expectation, we found that the measured quantum capacitance C_q decreases dramatically as disorder strength (controlled by the plasma-assisted Ag-cluster decoration[18]) increases. To understand the reduction in a quantitative way, here we proposed a two-parameter model which incorporates both the ADOS and its local fluctuations. Based on this model, we determined simultaneously the ADOS changes of the Ag-decorated graphene and the local fluctuations. It is found that ADOS indeed increase with disorder and follow the power law $\langle\rho(E_F)\rangle \sim |E_F|^{\alpha}$. The dramatic reduction of the measured C_q is caused by large fluctuations of LDOS, which follows a lognormal distribution and is independent of the Fermi energy.

Results

The fabrication of top-gate graphene devices and the measurement of capacitance are described in the method section. Fig. 1(a) schematically shows the geometry of the Ag-decorated graphene device with a top-gate. Fig. 1(b) illustrates the three-terminal configuration of the capacitance measurement $C_q(V_{ch})$ and oxide layer capacitance C_{ox}. In the serial connection, the quantum capacitance can be obtained from the top-gate capacitance C_{tg} through the relation $C_q(V_{ch}) = (C_{tg}(V_{tg})^{-1} - C_{ox}^{-1})^{-1}$. Here V_{ch} is the potential across the graphene sheet and can be obtained by integrating the charge conservation relation $C_{tg}(V_{tg})\cdot dV_{tg} = C_{ox}\cdot d(V_{tg} - V_{ch})$, i.e., $V_{ch} = V_{tg} - \int_0^{V_{tg}} \frac{C_{tg}}{C_{ox}} dV_{tg}'$. For pristine graphene devices, the quantum capacitance has been given by $C_{q0\_theory} = \frac{2e^2kT}{\pi(\hbar v_F)^2} \ln\left(2\left(1+\cosh\frac{eV_{ch}}{kT}\right)\right)$[11,13], where k denotes the Boltzmann constant and v_F the Fermi velocity. We fitted the measured quantum capacitance of pristine graphene C_{q0_exp} to the theory C_{q0_theory} to obtain $C_{ox} = 1.14\mu F/cm^2$. The result is shown in Fig. 1(c). The consistency in the vicinity of the NP has been improved compared to previous works[15,17,30]. One of the possible reasons for this improvement is the use of Cu mask before Yttrium deposition. By this way, we effectively reduced contamination from e-beam lithography, which may result in electron-hole puddles[30,31].

Fig. 1(d) shows the measured quantum capacitances $C_q(V_{ch})$ of three typical Ag-decorated graphene devices. Samples Ag1, Ag2 and Ag3 were decorated by Ag clusters via sputtering (5 W) for 1 s, 5 s and 10 s, respectively. Compared to the results recorded from the pristine graphene C_{q0_exp} in Fig. 1 (d), the quantum capacitance obtained from Ag-decorated graphene devices is much smaller. The $C_q(V_{ch})$ curves of Ag-decorated graphene devices are all asymmetrical between the electron and hole bands. This asymmetry was also observed in transport measurements[18]. As the Ag decoration is increased, the quantum capacitance of the devices decreases dramatically, which seems to be counterintuitive. Direct interpretation of these results via $C_q = e^2\cdot\langle\rho\rangle$ leads to disagreement with the theoretical predictions of the ADOS in disordered graphene.

In order to quantitatively understand the dramatic reduction of quantum capacitance in disordered graphene samples, we propose here a two-parameter model. In this model we incorporate both the ADOS of the disordered graphene and its LDOS fluctuations. To simulate the quantum capacitance, we first divide the total area A of graphene evenly into N small regions A_i, each has a size A/N as

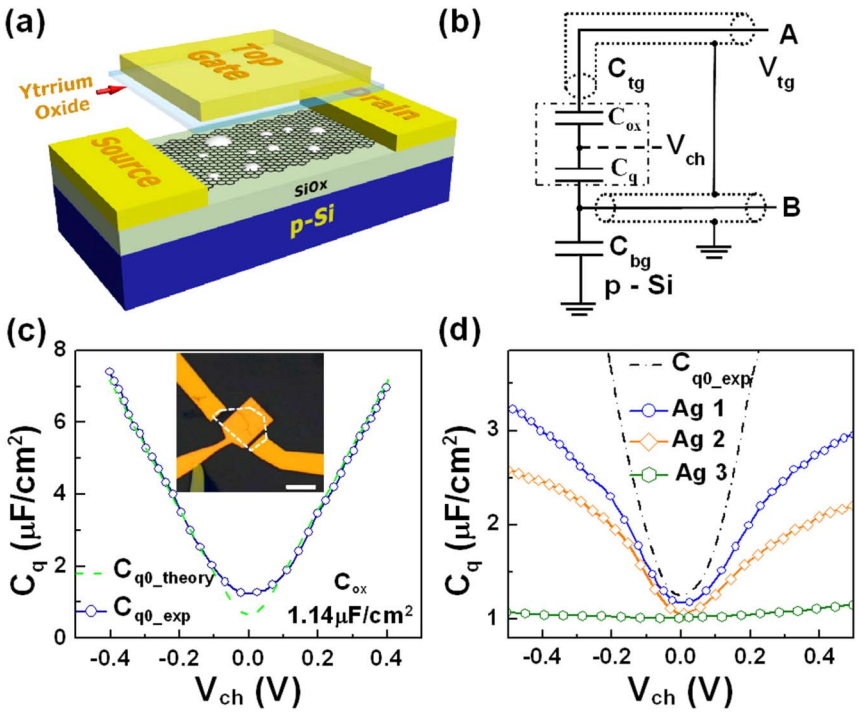

Figure 1 | (a) The geometry of a top-gate Ag-decorated graphene device. The small white islands represent the Ag clusters. (b) The equivalent circuit of the three-terminal capacitance measurement. The p-Si substrate is grounded to avoid its parasitic capacitance. (c) The quantum capacitance of one pristine graphene device with $C_{ox} = 1.14\mu F/cm^2$. The inset shows the optical image of the device. The dashed line indicates the outline of the graphene flake and the scale bar is 5 μm. (d) The measured quantum capacitance of three Ag-decorated graphene devices sputtered for 1 s, 5 s, and 10 s, respectively.

shown in Fig. 2(a). For simplicity, we set A = 1. In each region A_i, we define a normalized random variable $\delta_i = \frac{\rho_i}{\langle \rho_i \rangle}$ with $\langle \delta_i \rangle = 1$, where ρ_i is the LDOS in A_i and $\langle \rho_i \rangle$ is the ADOS of the system. For a given E_F, the local quantum capacitance in the region A_i can be written as

$$C_{qi} = e^2 \rho_i \cdot \frac{1}{N} = \frac{e^2}{N} \cdot \langle \rho_i \rangle \cdot \delta_i \quad (1)$$

As indicated by the equivalent circuit shown in Fig. 2(b), the total capacitance of the graphene device C_t is the summation of all parallel capacitances of N serial capacitances of C_o and C_{qi}, where $C_o = C_{ox}/N$ is the oxide layer capacitance in each small region. Thus, the quantum capacitance can be simulated using the following equation:

$$C_{q\_\mathrm{mod}} = \left(C_t^{-1} - (NC_o)^{-1}\right)^{-1} = \frac{N \sum_{i=1}^{N} C_{qi}/\left(C_{qi} + C_o\right)}{\sum_{i=1}^{N} 1/\left(C_{qi} + C_o\right)}, \quad (2)$$

which depends only on the ADOS $\langle \rho_i \rangle$ and the normalized distribution of δ_i. In order to simulate the quantum capacitance, we need to choose a correct distribution for $\delta_i = \frac{\rho_i}{\langle \rho_i \rangle}$. In strongly disordered graphene, the distribution of LDOS has been studied and found to be lognormal[34]. The lognormal distribution has also been evidenced experimentally in other 2D disordered materials[35]. Thus, to simulate Eq. (2), we propose a lognormal distribution for δ, i.e.,

$$f(\delta) = \frac{1}{\delta \cdot \sqrt{2\pi\xi^2}} \cdot \exp\left(-\frac{\left(\ln \delta + \xi^2/2\right)^2}{2\xi^2}\right), \quad (3)$$

or, $\delta \sim \ln \boldsymbol{N}\left(-\xi^2/2, \xi^2\right)$, $\delta \in [0, +\infty)$ with $\langle \delta \rangle = 1$. Because the variance of δ is $\exp\left(\xi^2\right) - 1$, ξ denotes the degree of the fluctuations. Theoretically, the ADOS in disordered graphene have been predicted to increase with disorder strength. One of the proposed analytical expressions for ADOS is a non-universal power law referred to quasiparticles in d-wave superconductor, which was supported by numerical exact diagonalizations (ED) for different types of disorders[3,4]. In our simulation, we assume that the ADOS $\langle \rho_i \rangle$ follow the non-universal power law. Thus, the ADOS at the Fermi energy ($E_F = eV_{ch}$) is given by

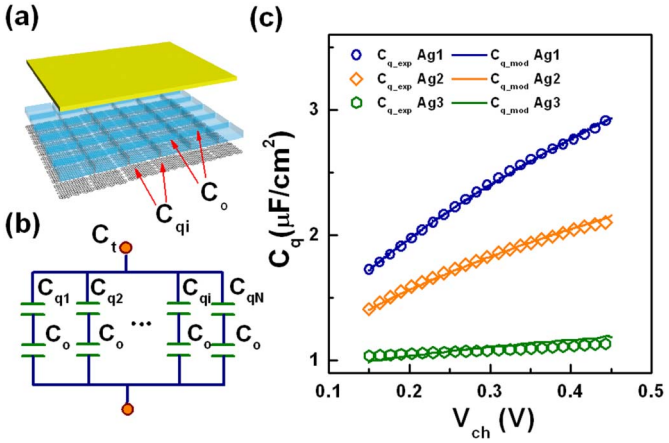

Figure 2 | (a) The top-gate Ag-decorated graphene device is divided into N small areas in the FLDOS model. C_o and C_{qi} are the oxide layer capacitance and the quantum capacitance in A_i, respectively. (b) Equivalent circuit of the top-gate graphene device in the FLDOS model. The total capacitance is the summation of parallel capacitances of all serial capacitances of C_o and C_{qi}. (c) The experimental quantum capacitance (scatters) and the simulation results by the FLDOS model (solid lines).

Table 1 | Fitting parameters and DOS at E_F = 0, 0.25 eV

Sample	α	ξ	ρ(0 eV) $eV^{-1}\,m^{-2}$	ρ(0.25 eV) $eV^{-1}\,m^{-2}$
Pristine [a]	1.00	0.00	0.00 [b]	2.77×10^{17}
Ag 1	0.74	1.66	3.36×10^{16}	7.25×10^{17}
Ag 2	0.69	1.95	9.73×10^{16}	9.22×10^{17}
Ag 3	0.49	2.75	7.43×10^{17}	2.41×10^{18}

[a]Only for comparison. [b] Vanishes at the NP.

$$\langle \rho_i \rangle = \rho_0(\alpha) + \frac{2e}{\pi(\hbar v_F)^2} \left(\frac{\lambda}{e}\right)^{1-\alpha} V_{ch}^{\alpha}, \quad (4)$$

where $\rho_0(\alpha) = \frac{32\lambda/t^2}{9\pi a^2(1-\alpha)} \exp\left(-\frac{1}{1-\alpha}\right)$ is the residual ADOS at NP, λ is the cut-off energy and $\lambda = 3t$, a is the lattice constant and t is the nearest-neighbor hopping energy[3,4] (t = 2.8 eV). The exponent $\alpha \in (0,1)$ in Eq. (4) represents the disorder strength, and its value decreases with increasing disorder strength.

The simulated quantum capacitance C_{q_mod} of Eq. (2) now depends only on two parameters: the disorder strength α and the degree of LDOS fluctuations ξ. By using Eq. (2), We performed Monte Carlo simulations and found that C_{q_mod} always converges to a well-defined value if N is sufficiently large for a chosen set of (α,ξ). In Fig. 2(c), we plot the simulated results for all the three disordered samples shown in Fig. 1(d). It shows good agreements between the simulated and measured quantum capacitance in a wide range of Fermi energies. To avoid ambiguity in the vicinity of the NP[30,31], the simulation started from V_{ch} = 0.15 V. Good agreements are also obtained for the hole branch. (see Supplementary Information). However, for Sample Ag3, some deviations between the measured and simulated results are noticed. This indicates that for a strongly disordered sample, the ADOS might deviate from the power law behavior of Eq. (4).

The fitting parameters for the three samples are listed in Table 1. It is clearly seen that α decreases with increasing disorder. The corresponding ADOS are plotted in Fig. 3(a), which shows explicitly that ADOS increases with disorder strength. This is consistent with the previous theoretical predictions of ADOS in disordered graphene[3,4] and our transport measurements[18]. Table 1 also indicates that the residual DOS ρ_0 at the NP cannot be ignored in such highly disordered graphene samples. Thus, the dramatic reduction in measured quantum capacitance found in Fig. 1(d) is caused by the large

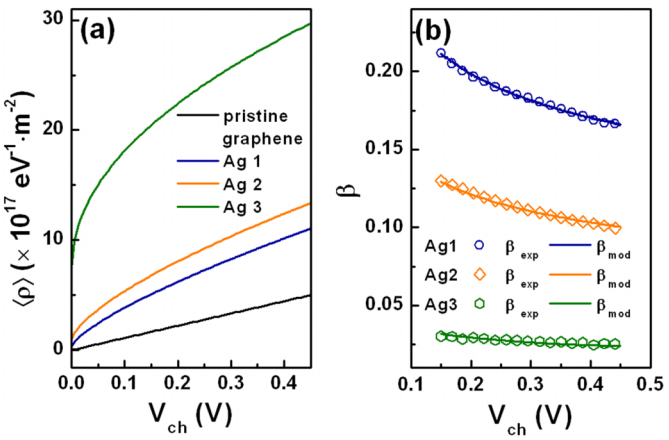

Figure 3 | (a) The simulated ADOS of three samples which follows Eq.(4) with α = 0.74,0.69,0.49 for Ag1, Ag2 and Ag3, respectively and the ADOS of pristine graphene for reference. (b) shows the reduction factor β of experimental (scatters) and simulation results by the FLDOS model (solid lines).

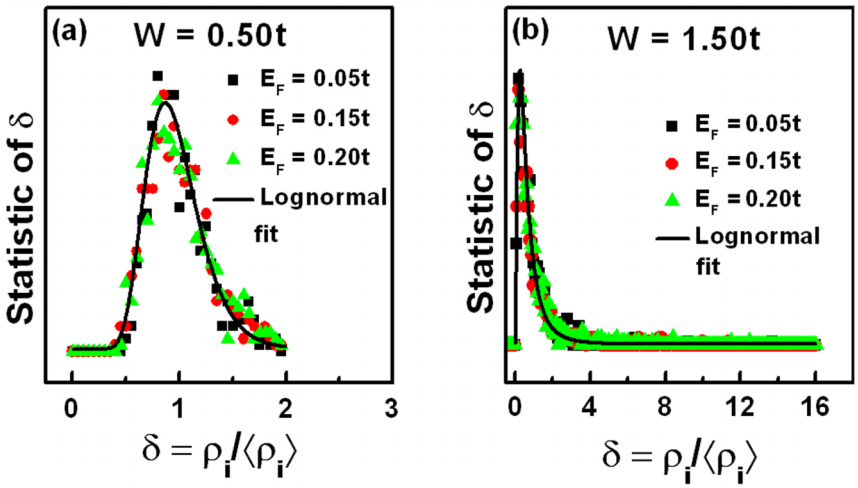

Figure 4 | (a) shows the distributions of normalized LDOS at $E_F = 0.05\ t$,0.15 t,0.20 t ($t = 2.8\ eV$), when $W = 0.50\ t$, which all follow one lognormal distribution. (b) also indicates the single lognormal distribution of LDOS at different E_F when $W = 1.50\ t$.

fluctuations of LDOS. Indeed, Table 1 shows that the value of ξ increases with disorder strength.

To quantify the reduction of quantum capacitance, here we define a dimensionless reduction factor $\beta = \frac{C_q}{C_{q^*}}$, where $C_{q^*} = \sum_i^N C_{qi} = e^2 \cdot \langle \rho_i \rangle \cdot \frac{1}{N} \cdot \sum_i^N \delta_i = e^2 \cdot \langle \rho_i \rangle$ is the quantum capacitance if the DOS is assumed to be uniform. Actually, C_{q^*} is also the real quantum capacitance of the disordered graphene. As we will show later that C_{q^*} can only be achieved when the oxide layer capacitance C_{ox} is much greater than C_{q^*}. In Fig. 3(b), we plot the reduction factor for both the measured quantum capacitance, i.e., $\beta_{\text{exp}} = C_{q\_\text{exp}}/C_{q^*}$, and the simulated quantum capacitance, i.e., $\beta_{\text{mod}} = C_{q\_\text{mod}}/C_{q^*}$. Here, $C_{ox} = 1.14 \mu F/cm^2$ for all three samples. It is clearly seen that more reduction is found for more disordered samples.

From the above simulation results, we would like to point out another interesting property of the LDOS fluctuations in disordered graphene. The fact that, for each disordered sample in Fig. 2(c) or 3(b), the quantum capacitance of disordered graphene can be excellently described by only two parameters in a wide range of Fermi energies indicates that the distribution of the normalized LDOS δ given in Eq. (3) is independent of E_F for a given disorder sample. To confirm this, we have performed the following simulations based on the Anderson tight-binding model for disordered systems[36]. We calculated the LDOS ρ_i in graphene with a given site disorder W by using the Haydock-Heine-Kelly recursion method. (see Supplementary Information for details). For two different values of W, the results of the distributions for three different values of E_F are shown in Figs. 4(a) and 4(b), where the hopping energy t is taken as the units of energy. These results show that for each given value of W, the distributions of δ at three different Fermi energies can all be described nicely by the same lognormal distribution (solid curve). It is also seen that the variance of the distribution is larger for larger W. Thus, these simulation results support our two-parameter model that the distribution of δ depends only on the disorder strength and is independent of the Fermi energy E_F.

Finally we would like to study the role played by the Yttrium oxide layer in the observed reductions of quantum capacitance of disordered graphene. The presence of a finite capacitance of the Yttrium oxide layer C_{ox} allows local fluctuations of channel potential across the graphene sheet in each small region. It is such fluctuations that lead to the reduction of the observed quantum capacitance of the graphene. For this purpose, we rewrite Eq. (2) in the following form:

$$\beta_{\text{mod}} = \frac{\langle \delta_i/(\delta_i + r) \rangle}{\langle 1/(\delta_i + r) \rangle}, \qquad (5)$$

where $r = \frac{C_{ox}}{C_{q^*}}$. In this form, Eq. (5) also exhibits an interesting scaling behavior, i.e., the reduction factor depends only on the ratio of C_{ox} to C_{q^*}, not on C_{ox} and C_{q^*} individually. Here we focus on one particular disorder strength and study the reduction factor as a function of r by using different thicknesses of the Yttrium oxide layer. We also test the r-scaling law by using data obtained at different Fermi energies, where C_{q^*} varies.

We measured the quantum capacitance of the same Ag-decorated graphene from devices with different C_{ox} by tuning the thickness of the Yttrium oxide layer. The decorations of all these samples were carried out simultaneously under the same conditions as Sample Ag1 in order to guarantee the same strength of disorder. The results of reduction factor for different Yttrium oxide layer thicknesses, which correspond to $C_{ox} = 1.13, 0.89, 0.76, 0.70 \mu F/cm^2$, and different Fermi energies ($V_{ch} = 0.15, 0.25, 0.35, 0.45\ V$) are shown in Fig. 5. All these data overlap nicely with the simulated solid curve obtained by using $\alpha = 0.74$, $\xi = 1.66$ shown in Table 1 for Sample Ag1. Fig. 5 verifies the r-scaling behavior of our two-parameter model with a lognormal distribution of LDOS. We also notice that the experimental data slightly deviates from the model when C_{ox} becomes

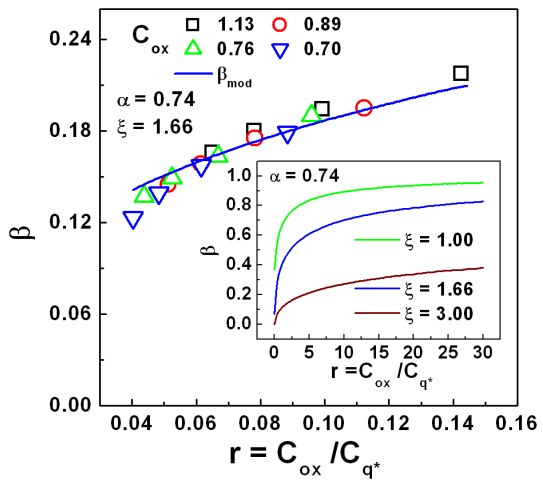

Figure 5 | The inset shows the reduction factor β (calculated by the FLDOS model) reaches 1 when C_{ox} is very large at different ξ. The reduction factor β (scatters) of graphene decorated by Ag for 1 s at 5 W with $C_{ox} = 1.13, 0.89, 0.76, 0.70 \mu F/cm^2$ agrees with the r-scaling of the FLDOS model (solid lines).

smaller. In this case, the oxide layer becomes thicker and the induced polarization effect might enhance the fluctuations of LDOS, leading to a smaller β. In the inset of Fig. 5, we show the β function obtained from different values of ξ. It is found that β decreases with increasing fluctuations of LDOS as expected. It also shows that β increases with r and saturates to 1 at very large r (unachievable practically), indicating that the real quantum capacitance $C_{q*} = e^2 \cdot \langle \rho \rangle$ of disordered graphene could only be achieved when $C_{ox} \gg C_{q*}$.

Discussion

Recently, experimental works demonstrated that the spatial LDOS fluctuations in the vicinity of the NP follow a Gaussian distribution[30,31]. Compared to the lognormal distribution which can describe LDOS in strongly disordered systems, the Gaussian distribution is only capable of describing systems with weak disorder. We have also performed simulations of Eq. (5) based on the Gaussian distribution. However, we do not found any significant reduction in quantum capacitance. (see Supplementary Information). In strongly disordered systems, the envelope of the localized wave functions decays exponentially from the center of the localization sites[36,37], creating strong spatial fluctuations of LDOS. This results in a dominance of LDOS at lower values than its mean and gives rise to a positive skewness. Although the variance of both Gaussian and lognormal distributions can represent the degree of fluctuations, the positive skewness of the lognormal distribution could be the underlying reason why it can correctly describe the LDOS fluctuations in disordered graphene, where significant LDOS fluctuations occur.

In conclusion, we have established a simple two-parameter(α,ξ) model for the quantum capacitance of disordered graphene. This model incorporates both the power-law dependence of the ADOS and the lognormal distribution of LDOS. By measuring the quantum capacitance of disordered graphene we simultaneously determine both the ADOS and its local fluctuations of the system. The model gives quantitative agreements with the measured quantum capacitance of three different strongly disordered Ag-decorated graphene samples. For Ag-decorated graphene samples, a given Ag-decoration corresponds to a configuration of disorder induced in the graphene sheet. The presence of disorder increases the ADOS and also induces large spatial fluctuations in LDOS compared to pristine graphene. The reduction of measured quantum capacitance is caused by large fluctuations of LDOS mediated by the presence of the insulating oxide layer. The validity of the model is also supported by our simulation results of LDOS using the Anderson model that the distribution of normalized LDOS is lognormal and independent of Fermi energy for a fixed disorder.

Methods

Device fabrication. The pristine graphene devices were prepared on p-Si substrates coated with 300 nm SiO_2 insulating layers, as reported previously[18]. The top-gate electrodes were then added using a standard e-beam lithography technique[17,38,39]. The insulating layer between the top-gate electrode and graphene was fabricated by depositing a thin layer of Yttrium on the graphene devices, followed by oxidation at 180°C for 10 min in air. We used a mask (thin Cu foils) in order to minimize the influence of direct electron beam irradiation[23] when patterning the insulating layer. The silver clusters were first deposited on the pristine graphene by the method reported previously[18]. Then, the graphene devices were immediately transferred into a high vacuum chamber for Yttrium deposition by electron-beam evaporation.

Capacitance measurement. The capacitance was measured by a Keithley CV analyzer (model 590) with a sensitivity of ~0.1fF. As illustrated in Fig. 1(b), the capacitance measurement was performed in a three-terminal configuration and the p-Si substrate was grounded to avoid its parasitic capacitance. The residual capacitance of the circuit in the same geometry of the devices without graphene is smaller than 0.3fF. The area of graphene for capacitance measurement was normally larger than 30 μm^2 as shown in the inset in Fig. 1(c). Pristine graphene devices were used to calibrate the capacitance of the Yttrium oxide layer (C_{ox}) of the Ag-decorated ones in the same batch. We extracted the quantum capacitance of a large number of devices for the same Ag decoration in different batches, and the results were similar.

1. Castro Neto, A. H., Guinea, F., Peres, N. M. R., Novoselov, K. S. & Geim, A. K. The electronic properties of graphene. *Reviews of Modern Physics* **81**, 109–162 (2009).
2. Das Sarma, S., Adam, S., Hwang, E. H. & Rossi, E. Electronic transport in two-dimensional graphene. *Reviews of Modern Physics* **83**, 407–470 (2011).
3. Dora, B., Ziegler, K. & Thalmeier, P. Effect of weak disorder on the density of states in graphene. *Physical Review B* **77**, 115422 (2008).
4. Ziegler, K., Dora, B. & Thalmeier, P. Density of states in disordered graphene. *Physical Review B* **79**, 235431 (2009).
5. Leconte, N. *et al.* Quantum transport in chemically modified two-dimensional graphene: From minimal conductivity to Anderson localization. *Physical Review B* **84**, 235420 (2011).
6. Hu, B. Y.-K., Hwang, E. H. & Das Sarma, S. Density of states of disordered graphene. *Physical Review B* **78**, 165411 (2008).
7. Wu, S. *et al.* Average density of states in disordered graphene systems. *Physical Review B* **77**, 195411 (2008).
8. Pereira, V. M., Guinea, F., Lopes dos Santos, J. M. B., Peres, N. M. R. & Castro Neto, A. H. Disorder Induced Localized States in Graphene. *Physical Review Letters* **96**, 036801 (2006).
9. Pereira, V. M., Lopes dos Santos, J. M. B. & Castro Neto, A. H. Modeling disorder in graphene. *Physical Review B* **77**, 115109 (2008).
10. Luryi, S. Quantum capacitance devices. *Applied Physics Letters* **52**, 501–503 (1988).
11. John, D. L., Castro, L. C. & Pulfrey, D. L. Quantum capacitance in nanoscale device modeling. *Journal of Applied Physics* **96**, 5180–5184 (2004).
12. Eisenstein, J. P., Pfeiffer, L. N. & West, K. W. Negative compressibility of interacting two-dimensional electron and quasiparticle gases. *Physical Review Letters* **68**, 674–677 (1992).
13. Fang, T., Konar, A., Xing, H. L. & Jena, D. Carrier statistics and quantum capacitance of graphene sheets and ribbons. *Applied Physics Letters* **91**, 092109.
14. Xia, J., Chen, F., Li, J. & Tao, N. Measurement of the quantum capacitance of graphene. *Nature Nanotechnology* **4**, 505–509 (2009).
15. Ponomarenko, L. A. *et al.* Density of States and Zero Landau Level Probed through Capacitance of Graphene. *Physical Review Letters* **105**, 136801 (2010).
16. Droscher, S. *et al.* Quantum capacitance and density of states of graphene. *Applied Physics Letters* **96**, 152104 (2010).
17. Xu, H. *et al.* Quantum Capacitance Limited Vertical Scaling of Graphene Field-Effect Transistor. *ACS Nano* **5**, 2340–2347 (2011).
18. Li, W. *et al.* Electron localization in metal-decorated graphene. *Physical Review B* **84**, 045431 (2011).
19. Moser, J. *et al.* Magnetotransport in disordered graphene exposed to ozone: From weak to strong localization. *Physical Review B* **81**, 205445 (2010).
20. Hong, X., Cheng, S. H., Herding, C. & Zhu, J. Colossal negative magnetoresistance in dilute fluorinated graphene. *Physical Review B* **83**, 085410 (2011).
21. Elias, D. C. *et al.* Control of Graphene's Properties by Reversible Hydrogenation: Evidence for Graphane. *Science* **323**, 610–613 (2009).
22. Gomez-Navarro, C. *et al.* Electronic transport properties of individual chemically reduced graphene oxide sheets. *Nano Letters* **7**, 3499–3503 (2007).
23. He, Y. H. *et al.* Modifying electronic transport properties of graphene by electron beam irradiation. *Appl. Phys. Lett.* **99**, 033109 (2011).
24. Bacsi, A. & Virosztek, A. Local density of states and Friedel oscillations in graphene. *Physical Review B* **82**, 193405 (2010).
25. Bena, C. Effect of a Single Localized Impurity on the Local Density of States in Monolayer and Bilayer Graphene. *Physical Review Letters* **100**, 076601 (2008).
26. Wehling, T. O. *et al.* Local electronic signatures of impurity states in graphene. *Physical Review B* **75**, 125425 (2007).
27. Xue, J. *et al.* Long-Wavelength Local Density of States Oscillations Near Graphene Step Edges. *Physical Review Letters* **108**, 016801 (2012).
28. Schnez, S. *et al.* Imaging localized states in graphene nanostructures. *Physical Review B* **82**, 165445 (2010).
29. Rutter, G. M. *et al.* Scattering and Interference in Epitaxial Graphene. *Science* **317**, 219–222 (2007).
30. Xu, H., Zhang, Z. & Peng, L. Measurements and microscopic model of quantum capacitance in graphene. *Appl. Phys. Lett.* **98**, 133122 (2011).
31. Martin, J. *et al.* Observation of electron-hole puddles in graphene using a scanning single-electron transistor. *Nature Physics* **4**, 144–148 (2008).
32. Lerner, I. V. Distribution functions of current density and local density of states in disordered quantum conductors. *Physics Letters A* **133**, 253–259 (1988).
33. Mirlin, A. D. Statistics of energy levels and eigenfunctions in disordered systems. *Physics Reports* **326**, 259–382 (2000).
34. Schubert, G., Schleede, J., Byczuk, K., Fehske, H. & Vollhardt, D. Distribution of the local density of states as a criterion for Anderson localization: Numerically exact results for various lattices in two and three dimensions. *Physical Review B* **81**, 155106 (2010).
35. Richardella, A. *et al.* Visualizing Critical Correlations Near the Metal-Insulator Transition in Ga1-xMnxAs. *Science* **327**, 665–669 (2010).
36. Anderson, P. W. Absence of Diffusion in Certain Random Lattices. *Physical Review* **109**, 1492–1505 (1958).

37. Lee, P. A. & Ramakrishnan, T. V. Disordered electronic systems. *Reviews of Modern Physics* **57**, 287–337 (1985).
38. Wang, Z. *et al*. Growth and Performance of Yttrium Oxide as an Ideal High-k Gate Dielectric for Carbon-Based Electronics. *Nano Letters* **10**, 2024–2030 (2010).
39. Xu, H. *et al*. Top-Gated Graphene Field-Effect Transistors with High Normalized Transconductance and Designable Dirac Point Voltage. *ACS Nano* **5**, 5031–5037 (2011).

Acknowledgments

The authors are grateful for fruitful discussions with Prof. Ho Bun Chan, Prof. Juhn-Jong Lin and Mr. Ieong Chao. Financial support from the Research Grants Council of Hong Kong (Project Nos. 604112, N_HKUST613/12, HKUST9/CRF/08) and technical support of the Raith-HKUST Nanotechnology Laboratory for the electron-beam lithography facility at MCPF (Project No. SEG_HKUST08) are hereby acknowledged.

Author contributions

W.L., X.L.C. and N.W. conceived and designed the experiments. W.L. and X.L.C. carried out the sample preparation, measurements and data analysis. W.L., ZQ.Z., P.S. and N.W. prepared the manuscript. All authors discussed and commented on the manuscript.

Additional information

Supplementary information accompanies this paper at http://www.nature.com/scientificreports

Competing financial interests: The authors declare no competing financial interests.

How to cite this article: Li, W. *et al*. Density of States and Its Local Fluctuations Determined by Capacitance of Strongly Disordered Graphene. *Sci. Rep.* **3**, 1772; DOI:10.1038/srep01772 (2013).